Asian Journal of Chemistry; Vol. 37, No. 12 (2025), 3019-3024
ASIAN JOURNAL OF CHEMISTRY
https://doi.org/10.14233/ajchem.2025.34647

Ferrioxalate Complex Derived Electrochemical Sensor for Nitrate and Phosphate Ions Detection

MAINAO JULI BASUMATARY, DIPJYOTI KALITA, RAJIB LOCHAN SARMA and JITUMANI RAJBONGSHI*

Department of Chemistry, Bhattadev University, Pathsala, Bajali-781325, India

*Corresponding author: E-mail: che.jitumani@bhattadevuniversity.ac.in

Received: 6 August 2025 *Accepted*: 1 October 2025 *Published online*: 30 November 2025 AJC-22190

Sensitive and selective sensing of nitrate and phosphate ions in aquatic environments is critical as their roles in eutrophication and potential hazards due to industrial and agricultural pollution. In this study, an electrochemical sensor using ferrioxalate, a complex routinely synthesized and discarded in undergraduate laboratories, is developed thus aligning with principles of green chemistry and waste valorisation. The metal-ligand coordination was confirmed by UV-Vis and FTIR spectroscopy showing characteristic stretching bands. The ferrioxalate complex was purified and used to modify a glassy carbon electrode. Electrochemical techniques, including cyclic voltammetry (CV) was employed to evaluate the complex's sensitivity and selectivity toward nitrate and phosphate ions. The sensor exhibited a sensitivity of -5.16×10^{-6} A/μM for nitrate ions with a limit of detection (LOD) of approximately 0.70 μM. While voltammetric peaks were clearly defined even at concentrations below this LOD, these signals represent qualitative detection and do not meet the statistical criteria for reliable quantification due to inherent measurement noise. The phosphate ions sensor showed higher sensitivity and a correspondingly lower LOD of 0.45 μM. The developed sensor demonstrated good linearity and was successfully applied to real water samples, highlighting its accuracy and reliability. This method offers a sustainable, cost-effective platform for water quality monitoring, effectively using the material into a functional green sensor.

Keywords: Ferrioxalate complex, Green chemistry, Electrochemical sensor, Nitrate ions, Phosphate ions, Cyclic voltammetry.

INTRODUCTION

Nitrate (NO_3^-) is an inorganic nitrogen ion, which acts as component of the nitrogen cycle in the natural world. Nitrate is a vital ingredient for the development and proliferation of plants. However, eutrophication due to its high quantities harm aquatic lives, its content in water needs to be closely monitored. Leaching of nitrogenous fertilizers from family lawns and agricultural applications from farms into water bodies is the primary source of the elevated NO_3^-concentration in water systems [1]. When aquatic plants and algae absorb nitrates from the water and overgrow, eutrophication results and accumulates high nitrate concentrations in these bodies [2]. Additional oxygen is depleted for other aquatic species by the overabundance of aquatic plants and the breakdown of these dead algae and plants in the water [3]. Humans are also at increased risk for methemoglobinemia (blue baby syndrome), hepatic encephalopathy and cancer when they consume water with a high nitrate content [4].

Again, phosphate (PO_4^{3-}) as a fundamental functional unit of DNA and RNA. In connection to the storage of genetic information, control of genes, energy transfer, processing of signals and contraction of muscles, phosphate ions are crucial [5]. In contrast, high phosphorus consumption can cause aquatic ecosystems to become eutrophic, which is followed by algae growth, breakdown and dissolved oxygen depletion [6,7]. For this reason, a lot of effort has gone into creating extremely sensitive and selective nitrate (NO_3^-) and phosphate (PO_4^{3-}) ions sensors for use in biological and environmental settings [8-10].

Traditional analytical techniques like ion chromatography, spectrophotometry and colorimetry, while accurate, often require expensive equipment and trained personnel [11,12]. On the other hand, electrochemical sensors are widely employed for the portable, selective and sensitive detection of various analytes due to their rapid response, high sensitivity and cost-effectiveness. A typical electrochemical sensor operates as a three-electrode system, comprising a working electrode (WE), reference electrode (RE) and counter electrode (CE), where the electrochemical reactions primarily occur at the working electrode.

Cyclic voltammetry (CV) is a key electrochemical technique for investigating the redox behaviour of analytes and

electrode materials. In electrochemical sensors, CV provides quantitative insight into electron transfer kinetics and peak potentials, enabling real-time detection of redox-active species. It also guides sensor optimization such as electrode modification and operational parameters enhancing sensitivity, selectivity and stability. Therefore, CV serves both as a fundamental analytical tool and a framework for designing high performance electrochemical sensors.

The ferrioxalate is a coordination compound of iron(III) with three oxalate ligands. Its redox-active properties make it an attractive candidate for various applications [13-18]. In fact, this complex exhibit strong electrocatalytic behaviour for NO_3^- and PO_4^{3-} ions which attribute to iron's redox versatility and the enhanced conductivity of the Fe oxalate complex [19-26]. The sharp responses observed in CV give insights into the potential and concentration dependent interactions, making this technique ideal for assessing detection limits and selectivity [27,28]. In this study, the working electrode is modified with ferrioxalate [$K_3Fe(C_2O_4)_3$] complex, which serves as a redox-active sensing material. The electrochemical behaviour of the sensor was investigated using cyclic voltammetry (CV) on a CHI600E electrochemical workstation. This study highlights the potential of this complex as an active sensing material, where its well-defined redox behaviour, ligand-to-metal charge transfer and interaction with target analytes can be exploited for sensitive and selective electrochemical detection.

EXPERIMENTAL

All chemicals *viz*. ferric chloride anhydrous, potassium hydroxide, potassium oxalate monohydrate, ethanol, *etc*. were used as received without further purification. The FTIR spectrum (Perkin-Elmer BXspectrometer, Shimadzu Corporation, Japan) of the synthesised ferrioxalate complex was recorded using the KBr pellet method. UV-Vis spectroscopy (SM-1600 Spectrophotometer) in aqueous medium revealed ligand-to-metal charge transfer and complexation-induced band shifts. Cyclic voltammetry, performed with a standard three-electrode setup using a glassy carbon electrode (GCE) modified with ferrioxalate complex as the working electrode, provided the electrochemical properties at pH 7.0

Synthesis of potassium tris(oxalato)ferrate(III) complex: Anhydrous iron(III) chloride (5 g) was dissolved in 20 mL of distilled water with continuous stirring until fully dissolved. Separately, potassium oxalate monohydrate (3 g) was dissolved in 20 mL of distilled water with thorough mixing and then mixed with the above prepared solution under constant stirring. The resulting greenish-yellow solution indicated the formation of $K_3Fe(C_2O_4)_3$ complex, which exhibited excellent electrocatalytic activity toward the electrochemical detection of nitrate and phosphate ions.

Electrochemical sensing of nitrate and phosphate: Electrochemical experiments were conducted using a CHI600E electrochemical workstation equipped with a three electrode system. A glassy carbon electrode (GCE) served as the working electrode (WE), a platinum wire as the counter electrode (CE) and an Ag/AgCl electrode as the reference electrode (RE). Prior to each measurement, the GCE was polished with alumina slurry, rinsed thoroughly with distilled water, and ultrasonically cleaned in ethanol and water (1 M each) for 10 min, followed by air drying. A 2 mg/mL ferrioxalate complex solution was prepared by ultrasonic dispersion in deionized water. For electrochemical sensing, 5 mL of this solution was mixed with 0.1 M NaCl electrolyte. Cyclic voltammetry (CV) was performed in the potential range of –1.0 V to +1.0 V at a scan rate of 20 mV s^{-1}. The supporting electrolyte for both nitrate and phosphate detection consisted of 10 mL of 0.1 M NaCl solution. Stock solutions of Na_2HPO_4 and KNO_3 (0.1 M each) were prepared in deionized water and incremental additions were prepared during sensing measurements.

Cyclic voltammetry was used to study the redox response of the ferrioxalate complex/GCE in the presence of nitrate and phosphate. Scans were recorded at varying concentrations of NO_3^- (0.0-2.5 μM) and PO_4^{3-} (0.10-2.25 μM). The effect of scan rate (0.1-0.9 V/s) and interference studies with phosphate were conducted to evaluate selectivity. Limit of detection (LOD) and linear range were calculated based on calibration plots.

RESULTS AND DISCUSSION

FTIR studies: The FTIR spectrum of the synthesized ferrioxalate complex was recorded in the range of 4000-400 cm^{-1}. The band assignments were correlated based on the previous infrared studies of similar metal–oxalate complexes [22,29-33]. The band observed at 538.71 cm^{-1} is attributed to the ν(Fe–O) stretching vibration. The oxalate ion exhibits a symmetric C–C stretching mode and an O–C–O deformation mode at 871.13 cm^{-1}. Four distinct oxalate stretching vibrations were identified at 1455.54, 2509 and 3423.80 cm^{-1}. Moreover, the broad band at 3430 cm^{-1} corresponds to the ν(O–H) stretching vibration, indicating the presence of lattice water molecules (Fig. 1).

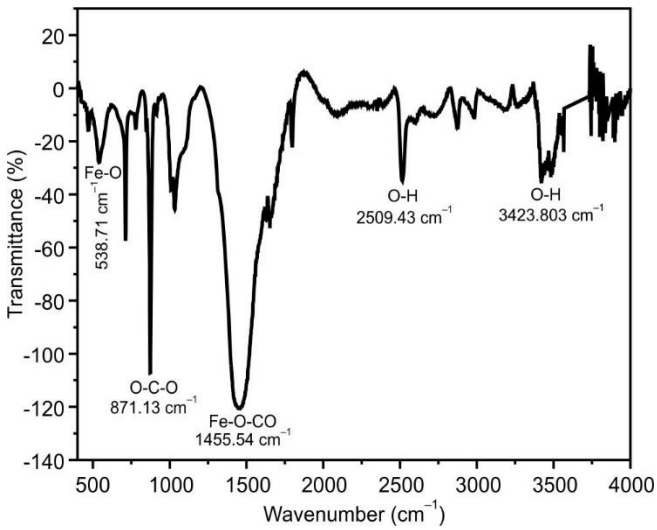

Fig. 1. FTIR spectrum of the synthesized $[Fe(C_2O_4)_3]^{3-}$ complex

UV-visible spectral studies: The UV-Vis absorption spectrum of the synthesized ferrioxalate complex was recorded in aqueous solution in the 200-700 nm range, providing the insights into its electronic transitions and interactions with ana-

lytes (Fig. 2). Two prominent absorption peaks were observed at 280 nm and 335 nm. The band at 280 nm is attributed to $\pi \rightarrow \pi^*$ transitions within the oxalate ligands, consistent with ligand-centered electronic excitations. The more intense peak at 335 nm is assigned to a ligand-to-metal charge transfer (LMCT) transition, in which electron density is transferred from the π-donor orbitals of the oxalate ligands to the empty *d*-orbitals of the Fe(III) center. No distinct *d*–*d* transitions were observed in the visible region, which is expected due to their spin- and Laporte-forbidden nature in high-spin d^5 octahedral complexes, resulting in very low molar absorptivity.

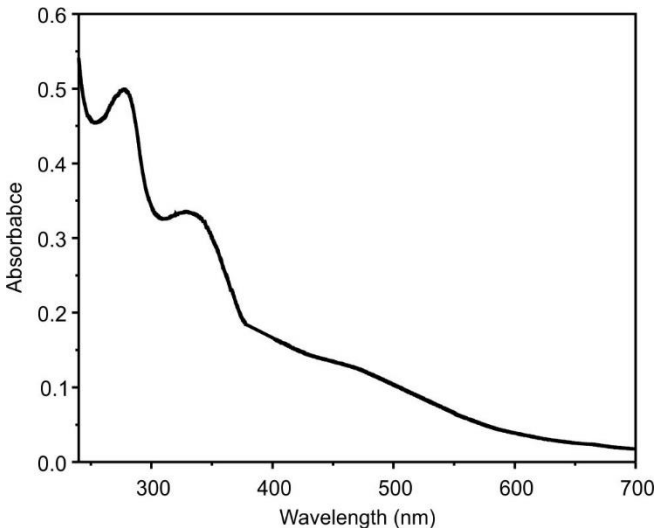

Fig. 2. UV-Vis absorption spectrum of $[Fe(C_2O_4)_3]^{3-}$ in aqueous solution

Electrochemical behaviour: The bare GCE showed no significant redox activity, while the ferrioxalate complex/GCE exhibited a well-defined redox couple in the potential range of –1 to +1 V. This is attributable to the Fe(III)/Fe(II) redox transformation process. Cyclic voltammetry of the ferrioxalate complex modified GCE was initially performed with different scan rates revealed a linear increase in peak current (I_p) with the square root of scan rate ($v^{1/2}$), indicating a diffusion-controlled electrochemical process as shown in Fig. 3.

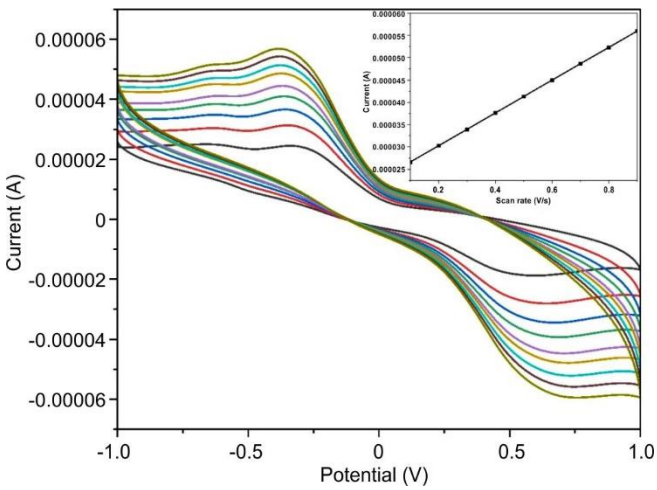

Fig. 3. Cyclic voltammograms of ferrioxalate complex modified GCE in NaCl (pH 7.0) at various scan rates (0.1–0.9 V/s) (Inset: linear relationship between peak current (I_p) and square root of scan rate ($v^{1/2}$)

Electrochemical behaviour in the presence of nitrate ions: As the nitrate concentration increased, both anodic and cathodic peak currents showed a distinct enhancement, indicating effective electrochemical interaction between nitrate ions and the ferrioxalate complex. This behaviour suggests that nitrate ions influence the redox activity of the complex, likely through coordination or electrostatic interactions at the electrode interface, thereby demonstrating its potential utility in the electrochemical sensing applications. As shown in Fig. 4, the cathodic peak current exhibited a linear relationship with nitrate concentration in the range of 0.25-2.5 μM, facilitating the development of a calibration curve.

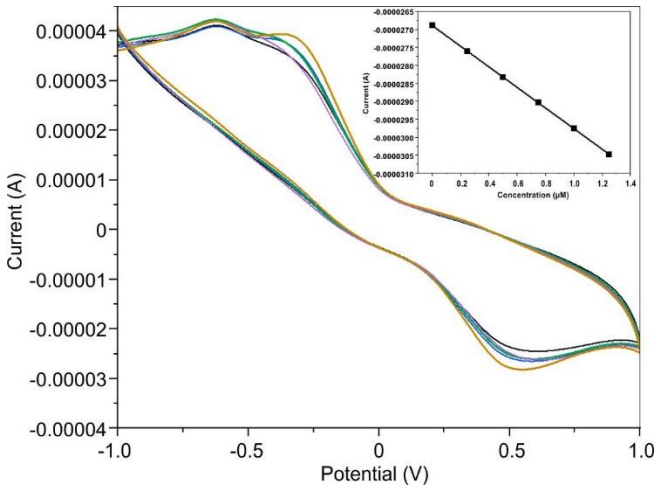

Fig. 4. Current response of the ferrioxalate complex/GCE sensor to increasing concentrations of nitrate (0.25-2.5 μM) in NaCl electrolyte (Inset: linear relationship between cathodic peak current (I_p) and nitrate concentration)

Phosphate ions sensing performance: The CV of the ferrioxalate complex modified GCE was initially performed in 0.1 M NaCl electrolytic solution without nitrate. The electrochemical behaviour of the oxalate ferrate complex was investigated in the presence of increasing concentrations of phosphate ions. A prominent feature of the CV response to phosphate (Fig. 5) is the absence of a distinct anodic peak at low concentrations, which becomes increasingly defined only upon successive additions. This suggests that at low PO_4^{3-} levels, the interaction between phosphate ions and the ferrioxalate complex is insufficient to significantly influence the electron transfer kinetics. However, upon further addition of phosphate beyond a certain concentration, a distinct secondary oxidation peak emerged at a more positive potential, while the original reduction peak gradually diminished in intensity. Simultaneously, the peak potentials exhibited a negative shift, suggesting a change in the redox mechanism or formation of a new electroactive species, likely due to the stepwise coordination or competitive binding of phosphate ions with the iron core.

The delayed appearance of the oxidation peak likely indicates a surface preconditioning effect, wherein higher analyte concentrations are required to promote adsorption or coordination processes that facilitate the redox reaction. This behaviour may also reflect a quasi-reversible or EC-type mechanism, where electron transfer is coupled with a slow chemical interaction that becomes electrochemically observable only beyond

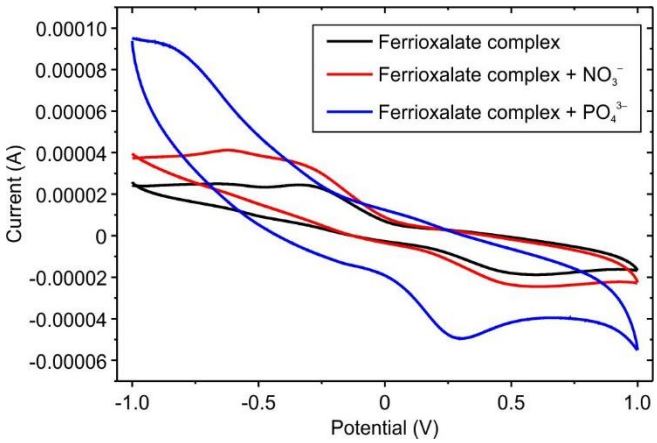

Fig. 5 Comparative current response of the ferrioxalate complex/GCE sensor to addition of NO_3^- and PO_4^{3-} ions in NaCl electrolyte

a threshold concentration. Such concentration-dependent peak emergence supports the hypothesis of a stronger, possibly site-specific, binding interaction between phosphate and the sensing layer.

Comparative electrochemical behaviour studies: The cyclic voltammetry revealed distinct behavioural differences between nitrate and phosphate ions sensing at the ferrioxalate complex-modified GCE. In pure NaCl electrolyte (Fig. 5), the electrode showed well-defined, symmetric redox peaks attributed to the Fe(III)/Fe(II) couple, with current proportional to the square root of scan rate, confirming a diffusion-controlled process. Upon nitrate addition (Fig. 5), the peak currents increased linearly without significant shape distortion or potential shift, suggesting an electrocatalytic enhancement with minimal surface alteration. This response supports a fast, diffusion-limited electron transfer process, where nitrate ions does not strongly adsorb or interfere with the electrode surface.

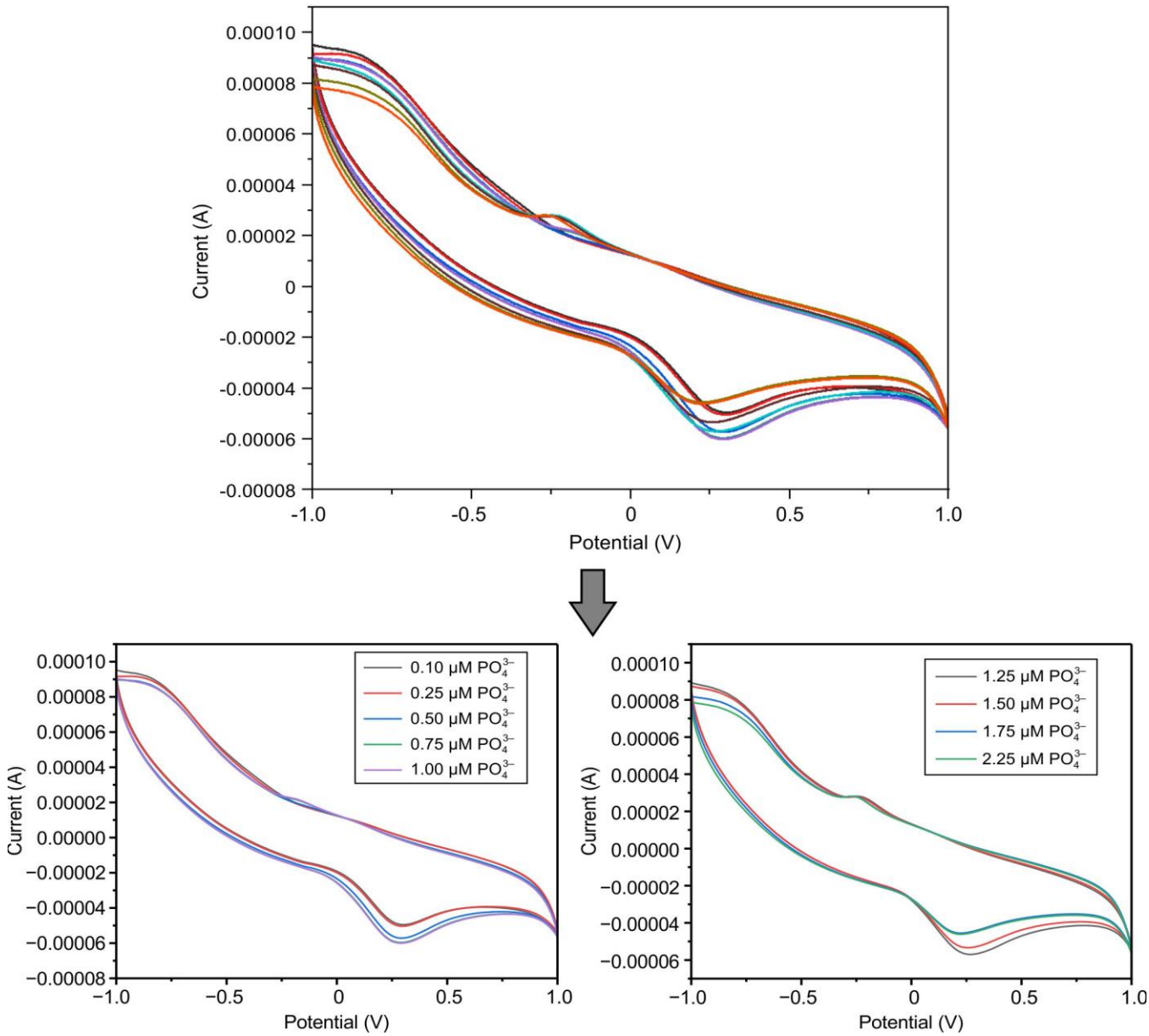

Fig. 6 Cyclic voltammograms of the ferrioxalate complex-modified GCE recorded in 0.1 M NaCl with increasing concentrations of PO_4^{3-} ions

In contrast, phosphate addition produced broader redox peaks and slight potential shifts, indicating a stronger or more complex interaction. Significantly, the anodic peak was not immediately visible at low phosphate concentrations and only became distinct at higher concentrations (Fig. 6). This delayed peak emergence suggests a surface preconditioning effect, where phosphate must accumulate or coordinate to the electrode before enabling observable oxidation. It may also reflect a quasi-reversible or EC-type mechanism, with slow chemical interaction preceding electron transfer. The phosphate-induced distortion and peak shift imply that this ion interacts more specifically or strongly with the sensing layer, potentially modifying the electrochemical interface.

The electrochemical sensor demonstrated effective detection capabilities for both nitrate and phosphate ions within their respective linear concentration ranges. For phosphate, the sensor exhibited a high sensitivity of -1.57×10^{-5} A/μM with a standard deviation of 2.16×10^{-6} A, using linear fit measured from 0 to 0.75 μM. This translated to a limit of detection (LOD) of 0.45 μM, indicating the capability of sensor to reliably quantify phosphate at sub-micromolar levels. In contrast, nitrate detection using linear fit over the range 0 to 1.25 μM showed a lower sensitivity of -5.16×10^{-6} A/μM, accompanied by a smaller standard deviation of 1.20×10^{-6} A. This resulted in a higher LOD of approximately 0.70 μM. While well-defined the voltammetric peaks were observed for nitrate even at concentrations below this LOD, these signals are considered qualitatively detectable but fall short of statistical reliability for quantitative analysis due to inherent measurement noise.

The comparatively higher sensitivity observed for phosphate ions detection accounts for its lower limit of detection (LOD), reflecting the sensor's enhanced responsiveness to phosphate ions within the tested concentration range. These results emphasize the importance of evaluating both sensitivity and measurement variability when assessing sensor performance as well as distinguishing between the qualitative detection capability and reliable quantification at low analyte levels.

Conclusion

This study presents the characteristic electrochemical activity of the ferrioxalate complex, $[K_3Fe(C_2O_4)_3]$, demonstrating its reversible redox behaviour and its potential as an efficient electrochemical sensor for the detection of nitrate and phosphate ions. The spectroscopic analyses (FTIR and UV-Vis) confirmed successful complex formation, while the cyclic voltammetry demonstrated distinct redox responses with high sensitivity, selectivity and reproducibility. The sensor exhibited a low detection limit and stable performance, highlighting its suitability for real-world water quality monitoring.

CONFLICT OF INTEREST

The authors declare that there is no conflict of interests regarding the publication of this article.

REFERENCES

1. R. Farina, G. D'Arrigo, A. Alberti, S. Scalese, G.E. Capuano, D. Corso, G.A. Screpis, M.A. Coniglio, G.G. Condorelli and S. Libertino, *Sensors*, **24**, 4501 (2024); https://doi.org/10.3390/s24144501.
2. M. Ballah, V. Bhoyroo and H. Neetoo, *J. Ecol. Environ.*, **43**, 5 (2019); https://doi.org/10.1186/s41610-018-0094-z
3. J.A. Camargo and Á. Alonso, *Environ. Int.*, **32**, 831 (2006); https://doi.org/10.1016/j.envint.2006.05.002
4. S.F. Johnson, *Curr. Probl. Pediatr. Adolesc. Health Care*, **49**, 57 (2019); https://doi.org/10.1016/j.cppeds.2019.03.002
5. W.E.G. Müller, H.C. Schröder and X. Wang, *Chem. Rev.*, **2019**, 12337 (2019); https://doi.org/10.1021/acs.chemrev.9b00460
6. C. Forano, H. Farhat and C. Mousty, *Curr. Opin. Electrochem.*, **11**, 55 (2018); https://doi.org/10.1016/j.coelec.2018.07.008
7. S. Cinti, D. Talarico, G. Palleschi, D. Moscone and F. Arduini, *Anal. Chim. Acta*, **919**, 78 (2016); https://doi.org/10.1016/j.aca.2016.03.011
8. A.S. Venkatadri, W.F. Wagner and H.H. Bauer, *Anal. Chem.*, **43**, 1115 (1971); https://doi.org/10.1021/ac60303a036
9. X. Chen, G. Zhou, S. Mao and J. Chen, *Environ. Sci. Nano*, **5**, 837 (2018); https://doi.org/10.1039/C7EN01160A
10. C. Warwick, A. Guerreiro and A. Soares, *Biosens. Bioelectron.*, **41**, 1 (2013); https://doi.org/10.1016/j.bios.2012.07.012
11. A.R. Marlinda, M.N. An'amt, N. Yusoff, S. Sagadevan, Y.A. Wahab and M.R. Johan, *Trends Environ. Anal. Chem.*, **34**, e00162 (2022); https://doi.org/10.1016/j.teac.2022.e00162
12. K. Lal, S.A. Jaywant and K.M. Arif, *Sensors*, **23**, 7099 (2023); https://doi.org/10.3390/s23167099
13. T. Fu and J. Tao, *Sens. Actuators B: Chem.*, **129**, 339 (2008); https://doi.org/10.1016/j.snb.2007.08.020
14. A. Saritha, B. Raju, D.N. Rao, A. Roychowdhury, D. Das and K.A. Hussain, *Adv. Powder Technol.*, **26**, 349 (2015); https://doi.org/10.1016/j.apt.2014.11.005
15. D. Bilanovic, R. E. Loewenthal, Y. Avnimelech, and M. Green, *Water SA*, **23**, 301 (1997).
16. A.A. Nogueira, B.M. Souza, M.W.C. Dezotti, R.A.R. Boaventura and V.J.P. Vilar, *J. Photochem. Photobiol. A: Chem.*, **345**, 109 (2017); https://doi.org/10.1016/j.jphotochem.2017.05.020
17. L.I. Doumic, P.A. Soares, M.A. Ayude, M. Cassanello, R.A.R. Boaventura and V.J.P. Vilar, *Chem. Eng. J.*, **277**, 86 (2015); https://doi.org/10.1016/j.cej.2015.04.074
18. B. Wriedt and D. Ziegenbalg, *ChemPhotoChem*, **5**, 947 (2021); https://doi.org/10.1002/cptc.202100122
19. A.L. Suherman, M. Lin, B. Rasche and R.G. Compton, *ACS Sens.*, **5**, 519 (2020); https://doi.org/10.1021/acssensors.9b02343
20. Y. Mai, K. Debruille, I. Mikhail, V. Gupta, E. Murray, R. Frantsuzov and B. Paull, *J. Sep. Sci.*, **48**, e70134 (2025); https://doi.org/10.1002/jssc.70134
21. S. Milardović, Z. Grabarić, V. Rumenjak and M. Jukić, *Electroanalysis*, **12**, 1051 (2000); https://doi.org/10.1002/1521-4109(200009)12:13<1051::AID-ELAN1051>3.0.CO;2-Z
22. A. Saritha, B. Raju, M. Ramachary, P. Raghavaiah and K.A. Hussain, *Physica B*, **407**, 4208 (2012); https://doi.org/10.1016/j.physb.2012.07.005
23. C. Visy, G. Bencsik, Z. Németh and A. Vértes, *Electrochim. Acta*, **53**, 3942 (2008); https://doi.org/10.1016/j.electacta.2007.07.060
24. A.A. Karyakin, *Electroanalysis*, **13**, 813 (2001); https://doi.org/10.1002/1521-4109(200106)13:10<813::AID-ELAN813>3.0.CO;2-Z
25. T. García, E. Casero, E. Lorenzo and F. Pariente, *Sens. Actuators B Chem.*, **106**, 803 (2005); https://doi.org/10.1016/j.snb.2004.09.033

26. M. Kundu, P. Krishnan, K.A. Chobhe, K.M. Manjaiah, R.P. Pant and G. Chawla, *J. Soil Sci. Plant Nutr.*, **22**, 2777 (2022); https://doi.org/10.1007/s42729-022-00845-5
27. F. Kivlehan, W.J. Mace, H.A. Moynihan and D.W. Arrigan, *Electrochim. Acta*, **54**, 1919 (2009); https://doi.org/10.1016/j.electacta.2008.06.046
28. S. Milardović, Z. Grabarić, M. Tkalčec and V. Rumenjak, *J. AOAC Int.*, **83**, 1212 (2000); https://doi.org/10.1093/jaoac/83.5.1212
29. M. Malathi, K. Vaishnavi, G. Ravi, M. Sunku and M. Vithal, *J. Solid State Chem.*, **276**, 133 (2019); https://doi.org/10.1016/j.jssc.2019.04.038
30. M. Narsimhulu and K.A. Hussain, *IOP Conf. Series Mater. Sci. Eng.*, **360**, 012048 (2018); https://doi.org/10.1088/1757-899X/360/1/012048
31. M.A. Gabal, *J. Mater. Res. Technol.*, **15**, 5841 (2021); https://doi.org/10.1016/j.jmrt.2021.11.012
32. A. Saritha, B. Raju and K.A. Hussain, *Adv. Sci. Lett.*, **19**, 885 (2013); https://doi.org/10.1166/asl.2013.4858
33. M.C. D'Antonio, A. Wladimirsky, D. Palacios, L. Coggiolaa, A.C. González-Baró, E.J. Baran and R.C. Mercader, *J. Braz. Chem. Soc.*, **20**, 445 (2009); https://doi.org/10.1590/S0103-50532009000300006